RevMexAA (Serie de Conferencias), **2**, 11-16 (1995)

HST FOC OBSERVATIONS OF η CARINAE [1]

G. Weigelt[2,3], R. Albrecht[2,4,5], C. Barbieri[2,6], J.C. Blades[2,7], A. Boksenberg[2,8], P. Crane[2,9], K. Davidson[10], J.M. Deharveng[2,11], M.J. Disney[2,12], P. Jakobsen[2,13], T.M. Kamperman[2,14], I.R. King[2,15], F. Macchetto[2,5,7], C.D. Mackay[2,16], F. Paresce[2,5,7], D. Baxter[7], P. Greenfield[7], R. Jedrzejewski[7], A. Nota[6,7], W.B. Sparks[7]

RESUMEN

Se usó la cámara FOC en el *HST* para observar regiones interiores de η Car. η Car es una LBV muy masiva con espectaculares eyecciones episódicas de capas a enorme tasa de pérdida de masa. Las imágenes de FOC resolvieron, en longitudes de onda visible y UV los 3 objetos speckle B, C, y D con separaciones de $\sim$ 0.1 a 0.3″. Se encontraron nuevas estructuras circunestelares. La imagen del objeto central A es más extensa que el núcleo de las correspondientes PSF. Se descubrió una nebulosidad en forma de anillo en las dos imágenes UV. Discutimos las observaciones y la naturaleza y movimiento de los objetos cercanos a la estrella dominante.

ABSTRACT

The Faint Object Camera (FOC) on the *HST* was used to observe the inner regions of η Carinae through the filters F550M, F307M, and F190M. η Carinae is a very massive LBV with spectacular episodic shell ejections at an enormous mass loss rate. The new high-resolution FOC images resolved for the first time at visible and UV wavelengths the 3 speckle objects B, C, and D at separations of $\sim$ 0.1 to 0.3″. In addition to these objects new circumstellar structures were found. The image of the central object A is more extended than the core of the corresponding PSF. In the two UV images a new ring-shaped nebulosity was discovered. We discuss the *HST* FOC observations, compare the *HST* images with the diffraction-limited speckle masking observations at near-IR wavelengths, and discuss the nature and motion of the objects near the dominant star.

Key words: **CIRCUMSTELLAR MATTER — STARS: INDIVIDUAL: (η CAR) — STARS: MASS LOSS**

[1]Based on observations with the NASA/ESA *HubbleSpaceTelescope*, obtained at the Space Telescope Science Institute, which is operated by AURA, Inc., under NASA contract NAS 5-26555.

[2]Member FOC Investigation Definition Team.
[3]Max-Planck-Institut für Radioastronomie, Auf dem Hügel 69, D-53121 Bonn, Germany.
[4]Space Telescope European Coordinating Facility, Karl-Schwarzschild-Strasse 2, D-8046 Garching, Germany.
[5]Astrophysics Division, Space Science Department of ESA.
[6]Osservatorio Astronomico di Padova, Vicolo Osservatorio 5, I-35122 Padova, Italy.
[7]Space Telescope Science Institute, 3700 San Martin Drive, Baltimore, MD 21218, USA.
[8]Royal Greenwich Observatory, Madingley Road, Cambridge CB3 0EZ, UK.
[9]European Southern Observatory, Karl-Schwarzschild-Str. 2, D-85748 Garching, Germany.
[10] Department of Astronomy, University of Minnesota, 116 Church St. S.E., Minneapolis, MN 55455, USA.
[11]Laboratoire d'Astronomie Spatiale du CNRS, Traverse du Siphon, Les Trois Lucs, F-13012 Marseille, France.
[12]Department of Physics, University College of Cardiff, P.O. Box 713, Cardiff CF1 3TH, Wales, UK.
[13]Astrophysics Division, Space Science Department of ESA, ESTEC, NL-2200 AG Noordwijk, The Netherlands.
[14]SRON - Space Research Utrecht, Sorbonnelaan 2, NL-3584 CA Utrecht, The Netherlands.
[15]Astronomy Department, University of California, Berkeley, CA 94720, USA.
[16] Institute of Astronomy, Madingley Road, Cambridge CB3 0HA, England, UK.

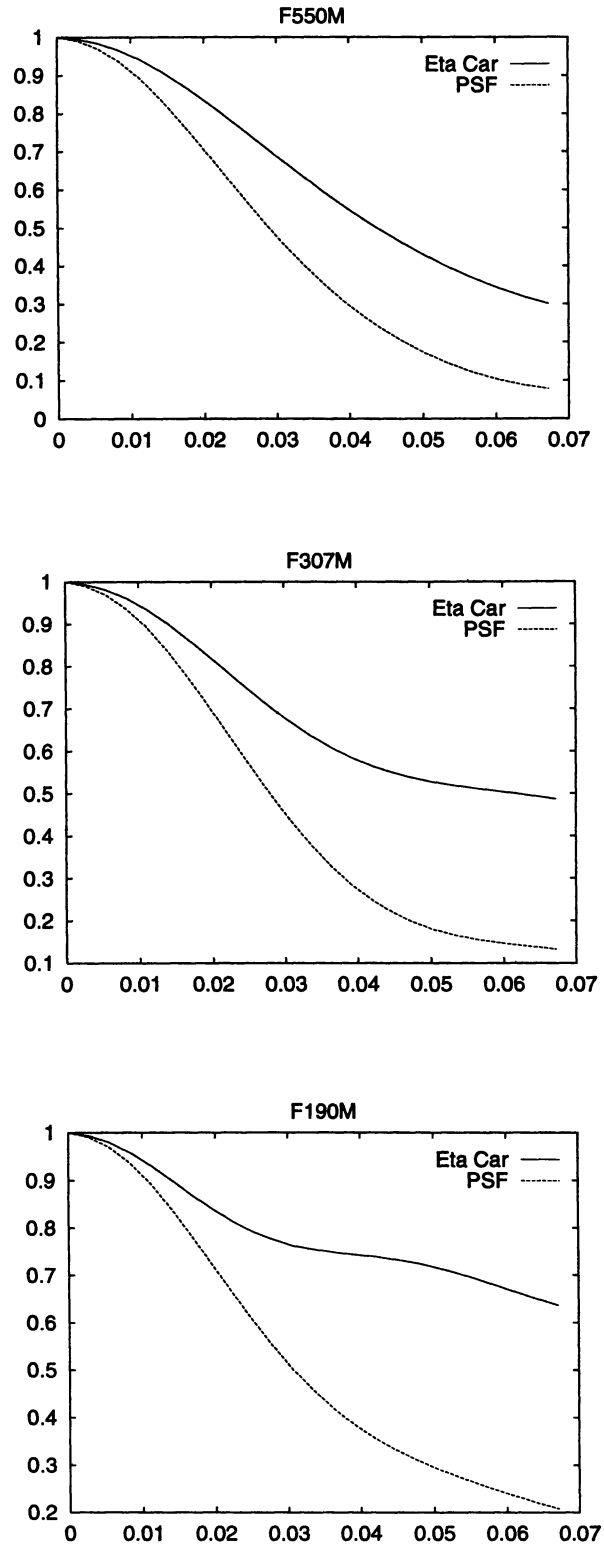

Fig. 2. Intensity plots of the azimuthal averages of the dominant A-component in the images 1a to 1c and of the corresponding point spread functions (from top to bottom: F550M, F307M, and 190M; the abscissas are labelled in arcsec).

1. INTRODUCTION

η Carinae is the most extreme, eruptively unstable Luminous Blue Variable, with enormous, sporadically variable mass loss at velocities ranging from 300 to 1400 km s^{-1} (Andriesse, Donn, & Viotti 1978; Hyland et al. 1979; Davidson et al. 1986; White et al. 1994; Walborn, Blanco, & Thackery 1978; Viotti et al. 1986, 1989; Hillier & Allen, 1992; Meaburn et al. 1993a, 1993b). It is one of the most massive and luminous stars in the Galaxy (see van Genderen & Thé 1985; Davidson 1987, 1989; and many references cited therein). Its distance is 2300–2800 pc (Feinstein, Marraco, & Muzzio 1973; Walborn 1973; Thé, Bakker, & Antalova 1980) and its bolometric absolute magnitude is close to -12. η Car is surrounded by the "Homunculus" compact nebula, which consists of material ejected from the star during its strong eruption observed in the years 1830–1860. The ejected material is nitrogen-rich (Davidson et al. 1986), showing that the star is evolved and not a pre-main sequence object. Therefore η Carinae represents a unique opportunity to study the evolution of a very massive star at an important and short-lived unstable phase of its evolution, most likely the pre-Wolf-Rayet stage (Maeder 1989). Speckle interferometry and speckle masking observations of η Carinae (in particular, the bright "core" in the Homunculus) have resolved a dominant object and three other compact objects at separations 0.114″ , 0.177″, and 0.211″ (Weigelt & Ebersberger 1986; Hofmann & Weigelt 1988). The three fainter objects were unexpected, and their nature is puzzling and difficult to interpret. Since the speckle observations were restricted to long wavelengths ($\sim$ 8500 A), observations at visual and UV wavelengths are also needed. Here we report such observations obtained with the *HST* Faint Object Camera.

2. OBSERVATIONS AND ANALYSIS

η Carinae was observed on 10 Oct. 1991 and on 3 Nov. 1992 with the f/96 camera of the *HST* Faint Object Camera. Three exposures were taken with the filter combinations: F190M+F175W+F4ND (exposure time 2400 s, 10 Oct. 1991), F307M+F342W+8ND (2000 s, 10 Oct. 1991), and F550M+F6ND (2400 s, 3 Nov. 1992).

The ND filters are neutral density filters. The F190M, F307M, and 550M filters of the f/96 camera have peak transmission at 1990 A, 3070 A, and 5460 A, respectively. The W-filters (W = wide band) are blocking filters. Therefore, the peak transmission of the filter combinations is approximately equal to the peak transmission of the M-filters (M = medium band) mentioned above. The FOC is described in detail in Macchetto et al. (1980) and Paresce (1990).

Based on data from the *HST* Faint Object Spectrograph (Davidson et al. 1995), we estimate that the F550M and F307M images represent mainly continuum light plus small contributions by Fe II and [Fe II] emission lines. Bright Fe III emission near 1900 A probably contributed 10–15 % of the light in the F190M image. The F307M image includes roughly the same wavelengths as the *HST* /PC images shown by Ebbets et al. (1992, 1994).

Figure 1 (Plate 1) shows the inner 64 × 64 pixels ($\sim$ 1.4″ × 1.4″) of the F190M, F307M, and F550M images obtained after flat-fielding, distortion correction and compensation (filtering) of the fixed pattern noise from the detector. In the F550M image the dominant central object, the three speckle objects, and additional nebulosity can be seen. As noted above, this is essentially a continuum-light image. Since it closely resembles the speckle images, we conclude that the speckle results were not qualitatively perturbed by peculiar emission features near 8500 A. In the F307M and F190M images a curious ring-shaped nebulosity is very bright. The F307M and F190M images look more diffuse than the F550M image since scattering by dust is stronger in the UV. The contrast of the images is low because of the spherical aberration of the telescope.

Figures 2a to 2c are azimuthal averages of the dominant A-component of the images 1a to 1c and of the corresponding point spread functions. The plots show that at all three wavelengths the image of the A-component is more extended than the core of the corresponding point spread functions.

Figure 3a is a contour plot of the inner 32 × 32 pixels ($\sim$0.7″ × 0.7″) of Fig. 1a and Fig. 3b is a Richardson-Lucy restoration of the inner 32 × 32 pixels of Fig. 1a.

A comparison of Fig. 1a with the speckle masking image observed in 1985 (Hofmann & Weigelt 1988) shows that the proper motion of the three speckle objects can be derived from the two images. In the F550M FOC image the projected separations and position angles of the objects B, C, and D are: 0.123″ /334.0°, 0.208″ /304.0°, and 0.241″ /336.0°, respectively.

The corresponding separations and position angles of the 1985 speckle observations are: 0.114″ /340.0°, 0.177″ /296.5°, and 0.211″ /335.5°.

Object B cannot be used for a reliable motion measurement since its distance to the the central object is

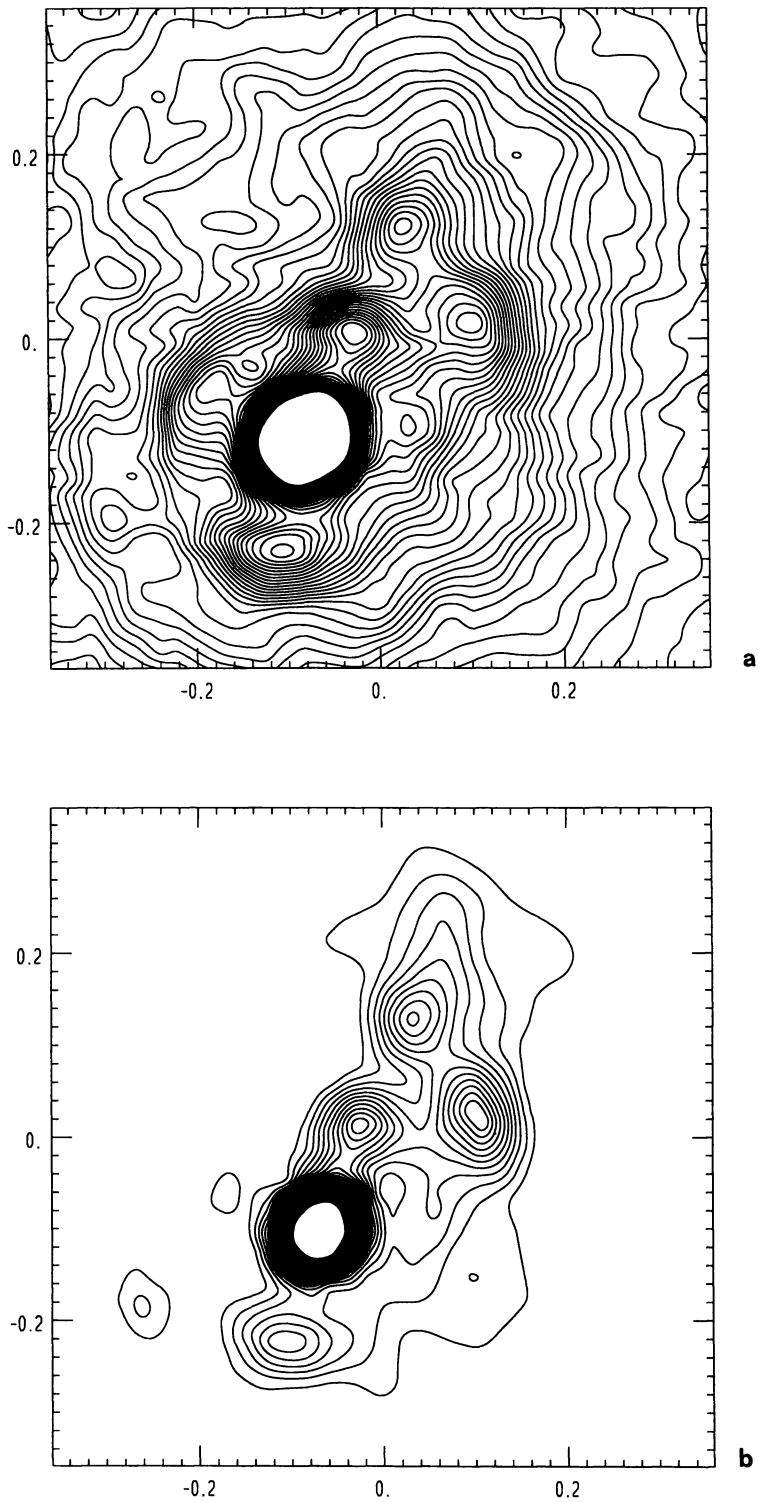

Fig. 3. (a) Contour plot of the inner 32 × 32 pixels ($\sim 0.7'' \times 0.7''$) of Fig. 1a (550M raw image) and (b) Richardson-Lucy restoration of the 550M image (80 iterations). In each panel the contour levels are plotted from 3 to 50% of the peak intensity in steps of 1%, and the axes are labelled in arcsec. North is at the top and east to the left.

too small. The increase rates of the projected separations A-C and A-D are about 0.031″ /7.8 years and 0.030″ /7.8 years, respectively, corresponding to velocities of about 0.031 × 2500 AU/7.8 yr ≈ 47.1 km s^{-1} and about 45.6 km s^{-1} if the distance is 2500 pc. However, the error of this first velocity determination is probably quite high since the speckle observation was made at a wavelength of ∼8500 A and the *HST* observation was made at ∼5500 A. If these proper motions are approximately correct, the simplest interpretation is that components C and D were thrown out from the star at some time between 1880 and 1930. Perhaps they were ejected in the outburst seen around 1890 (see Walborn & Liller 1977).

The relative intensities B/A, C/A, and D/A of the objects B, C, and D are difficult to measure because of the spherical aberration. We measured the intensity ratios in the raw images (Figs. 1a-c) and in all intensity measurements we calculated averages over 3 × 3 pixels. First the count numbers at positions A to D were determined. Then the ratios of the intensities at all positions in the wings of a single-star point spread function (from a psf calibration measurement) and the intensity in the center of the single-star psf were determined. These psf intensity ratios were used to correct approximately the influence of the psf wings of A to D on the photometry and to determine improved B/A, C/A, and D/A values. For the F550M image we obtained for B/A, C/A, and D/A approximately 0.36, 0.34, and 0.32, respectively (for the F307 and F190 images the same ratios B/A, C/A, and D/A are approximately 0.54, 0.62, 0.62 and 0.69, 0.74, 0.76, respectively).

3. DISCUSSION

Davidson & Humphreys (1986) discussed the possibility that the three speckle objects B, C, D could be stars or perhaps compact nebular objects. Both alternatives were found to present theoretical difficulties. If the objects have rapid proper motions as we suspect (see above), then they are probably gas clouds ejected from the primary star. *HST*/FOS spectroscopy supports this interpretation; component A has the spectrum of a star with a very strong wind, while components B, C, and D apparently produce forbidden emission lines and show no signs of stellar features other than those seen in object A (Davidson et al. 1995). However, objects B, C, D are surprisingly bright relative to A, for example, about 30 – 40% of the illuminating object A at 5500 A in spite of the small angular diameter of C or D. One possible explanation is that the dominant star is surrounded by a compact, equatorial dust disk or dust ring (annulus). If we assume that we see the equatorial dust disk nearly edge-on, then the central star could be very much obscured for an observer on earth, but the objects B to D could be in the undisturbed illuminating light cone from the central star. The illumination of objects B to D is strongest if B to D are located in polar direction, which is probably the direction of the two homunculus lobes. But B to D could also be part of a large equatorial dust plane between the two homunculus lobes. In either case, they probably reflect some light from the star itself (object A), because they have strong continua in the FOS data mentioned above.

Another very interesting structure is the very compact circumstellar object with diameter ≤ 0.05″ (≤ 125 AU) surrounding the star or in front of the star (see Fig. 2). Because of this object we probably cannot see the surface of the central star directly but we see the surface of an optically thick shell or wind around the star. This circumstellar object could also be part of the equatorial dust disk discussed above.

4. SUMMARY

HST FOC observations of η Carinae have for the first time resolved the speckle objects B to D at visible and UV wavelengths, as well as additional nebulosity. The *HST* observations also show that the central object η Car A is surrounded by a circumstellar object with diameter ≤ 0.05″ (≤ 125 AU). By comparing the speckle masking observations in 1985 with the FOC observations in 1992, the proper motion of C and D was determined for the first time. The high relative brightness of the three speckle objects B to D can be explained if we assume that for an observer on earth the illuminating central star is obscured by a dust disk, whereas B, C, and D are in the bright illuminating light cone from the central star.

D. Baxter, P. Greenfield, R. Jedrzejewski, and W.B. Sparks acknowledge support from ESA through contract 6500/85/NL/SK. J.C. Blades, P. Crane and I.R. King acknowledge support from NASA through contracts NAS5-1733, NAS5-27760 and NAS5-28086. G. Weigelt acknowledges support from the German Space Agency (DARA) through contract 50OR9204 and wants to thank T. Reinheimer, D. Schertl, M. Schreiner, and S. Schäfer for their very valuable help during data processing.

REFERENCES

Andriesse, C.D., Donn, B.D., & Viotti, R. 1978, MNRAS, 185, 771
Davidson, K. 1987, Instabilities of Luminous Early Type Stars, ed. H. Lamers & C. de Loore (Dordrecht: Reidel), p. 127
_____. 1989, Physics of Luminous Blue Variables, ed. K. Davidson, A. Moffat, & H. Lamers (Dordrecht: Kluwer), p. 101
Davidson, K., & Humphreys, R.M. 1986, A&A, 164, L7
Davidson, K., Dufour, R.J., Walborn, N.R., & Gull, T.R. 1986, ApJ, 305, 867
Davidson, K. et al. 1995, in preparation
Ebbets, D., White, R., Walborn, N., Davidson, K., & Malumuth, E. 1992, in Science with the Hubble Space Telescope, Proc. ESO Conf. No. 44, ed. P. Benvenuti & E. Schreier (Garching: ESO), p. 395
Ebbets, D., Garner, H., White, R., Davidson, K., Malumuth, E., & Walborn, N. (1994) in Circumstellar Media in the Late Stages of Stellar Evolution, Proc. 34th Herstmonceux Conf. ed. R.E.S. Clegg, I.R. Stevens, & W.P.S. Meikle (Cambridge: Cambridge U. Press), p. 95
Feinstein, A., Marraco, H.G., & Muzzio, J.C. 1973, A&AS, 12, 331
Hyland, A.R., Robinson, G., Mitchell, R.M., Thomas, J.A., & Becklin, E.E. 1979, ApJ, 233, 145
Hillier, D.J., & Allen, D.A. 1992, A&A, 262, 153
Hofmann, K.-H., & Weigelt, G. 1988, A&A, 203, L21
Macchetto, F., van de Hulst, H. C., di Serego Alighieri, S., & Perryman, M.A.C. 1980, The Faint Object Camera for the Space Telescope (Noordwijk: ESTEC) ESA SP-1028
Maeder, J. 1989, IAU Coll. 113, Physics of Luminous Variables, ed. K. Davidson, A.F.J. Moffat, & H.J.G.L.M. Lamers (Dordrecht: Kluwer)
Meaburn, J., Gehring, G., Walsh, J.R., Palmer, J.W., López, J.A., Bryce, M., & Raga, A.C. 1993a, A&A, 276, L21
Meaburn, J., G., Walsh, J.R., & Wolstencroft, R.D. 1993b, A&A, 268, 283
Paresce, F., 1990, Faint Object Camera Instrument Handbook, Version 2.0 (Baltimore: Space Telescope Science Institute)
Thé, P.S., Bakker, R., & Antalova, A. 1980, A&AS, 41, 93
van Genderen, A.M., & Thé, P.S. 1984, Space Sci. Rev., 39, 317
Viotti, R., Rossi, L., Altamore, A., Rossi, C., & Cassatella, A. 1986, in IAU Symp. 116, Luminous Stars and Associations in Galaxies, ed. C.W.H. de Loore, A.J. Willis, & P. Laskarides (Dordrecht: Reidel), p. 249
Viotti, R., Rossi, L., Cassatella, A., Altamore, A., & Baratta, G.B. 1989, ApJS, 71, 983
Walborn, N.R. 1973, ApJ, 179, 517
Walborn, N.R., Blanco, B.M., & Thackery, A.D. 1978, ApJ, 219, 498
Walborn, N.R., & Liller, M.H. 1977, ApJ, 211, 181
Weigelt, G., & Ebersberger, J. 1986, A&A, 163, L5
White, S.M., Duncan, R.A., Lim, J., Nelson, G.J., Drake, S.A., & Kundu, M.R. 1994, ApJ, 429, 380

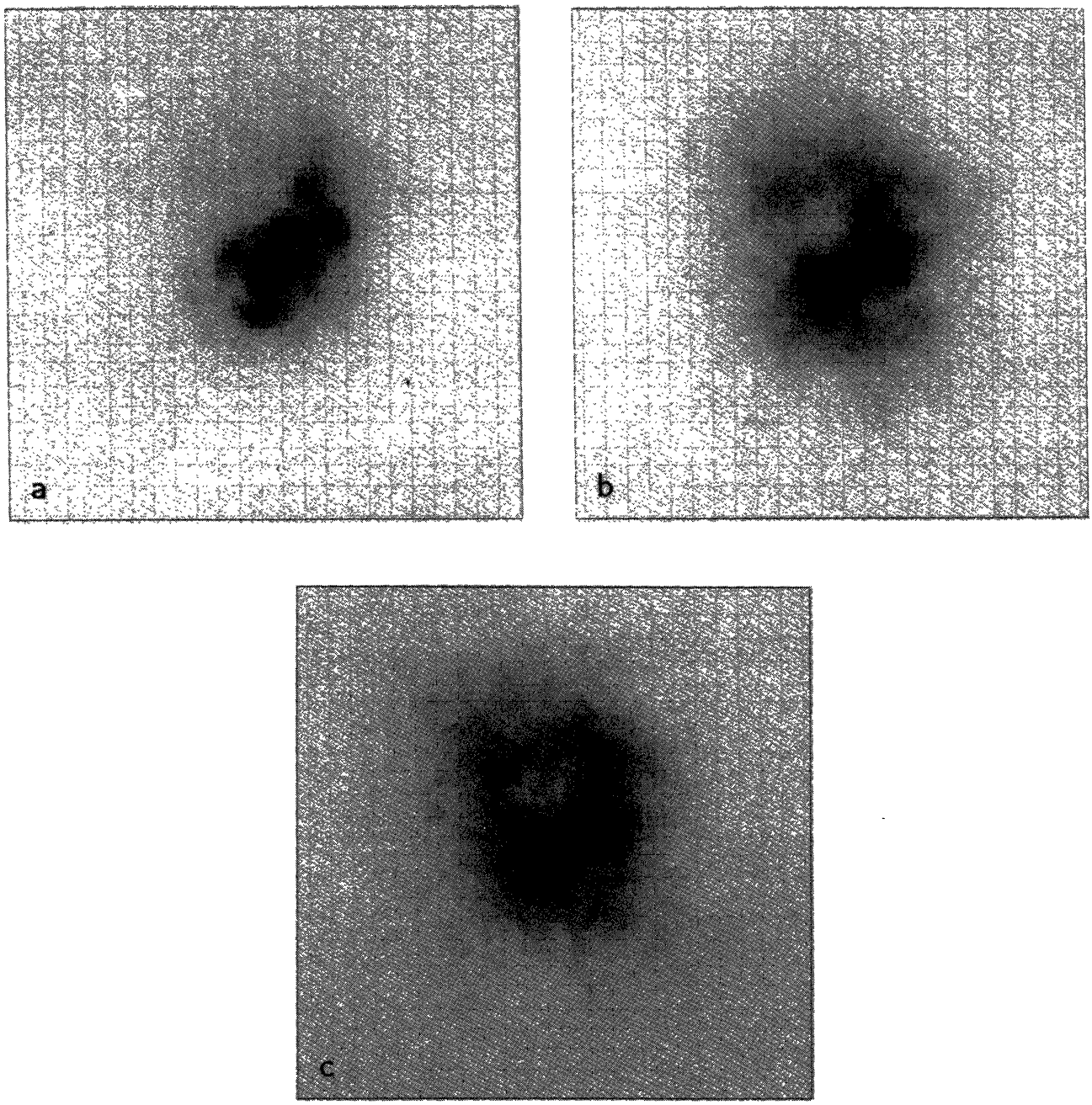

Fig. 1. Negative grey-scale representation of the inner $\sim 1.4''$ $\times$ $1.4''$ (64×64 pixels) of the *HST* FOC raw images of η Carinae taken through the filter (a) F550M, (b) F307M + F342W, and (c) F190M + F175W. North is at the top and east to the left.